

Theory of interstitial transition-metal impurities in silicon

Gary G. DeLeo, George D. Watkins, and W. Beall Fowler

Department of Physics, Lehigh University, Bethlehem, Pennsylvania 18015

(Received 30 September 1980)

The electronic structure of interstitial iron-group transition-metal impurities in silicon is calculated by the spin-restricted scattered-wave $X\alpha$ method. A representation of pure crystalline silicon is provided by the cluster $\text{Si}_{10}\text{H}_{16}$, which is centered on the high-symmetry (T_d) interstitial position. The sixteen hydrogen atoms serve to terminate the cluster by tying up the dangling bonds. The neutral transition-metal impurities, Cr, Mn, Fe, Co, and Ni, are placed at the center of this cluster. The results of the calculation indicate that the transition-metal $3d$ states interact primarily with t_2 and e states of the $\text{Si}_{10}\text{H}_{16}$ cluster which are located near the top of the valence band. Consequently, antibonding t_2 and e states are pushed into the band gap for Cr, Mn, Fe, and Co with t_2 below e ; the interaction with the $3d$ state of Ni is relatively weak. Partially occupied levels in the band gap are known to be electrically active and the results of the present calculation are in good agreement with the electron paramagnetic resonance experiments of Ludwig and Woodbury.

I. INTRODUCTION

The electronic properties of semiconductors are modified by the presence of both substitutional and interstitial $3d$ transition-metal impurities. For a wide variety of these elements and in a surprisingly large number of charge states, energy levels are produced deep within the band gap. Evidence for this effect in silicon comes primarily from the electron paramagnetic resonance (EPR) experiments of Ludwig and Woodbury.¹ These experiments indicate that the interstitial position is favored over the substitutional position for the iron-group transition-metal elements in silicon. In fact, iron-group transition-metal ions covering five columns of the Periodic Table have been found to be electrically active as interstitials. An understanding of the chemical trends associated with these transition-metal impurities emerges from these observations. A rigorous theoretical calculation is essential if this understanding is to be verified and extended. The single theoretical calculation which has been performed for the interstitial² gives results in disagreement with the observations of Ludwig and Woodbury.

The deep-level impurities in semiconductors have been treated successfully by a number of theoretical methods.³⁻¹¹ These approaches fall into two categories: perturbative and cluster. The starting point for the perturbative approach is the band structure of the perfect solid, usually contained in a Green's function. The effect of the impurity is treated as a localized perturbation. Quite recently, this approach has been made tractable by the introduction of localized orbitals, which represent the Green's function and the effects of the impurity potential.^{3,4} This technique

has been successfully applied to the study of vacancy levels in Si (Refs. 3 and 4) and GaP.¹¹ The transition-metal impurities have not been treated by this method.

In the cluster approach, a finite set of atoms is assumed to provide an adequate representation of the solid, particularly in the region about the defect. Quantum chemistry provides a variety of techniques suitable for calculating the electronic structure of these molecular clusters. Extended Hückel theory was employed in the study of deep levels in covalent solids by Messmer and Watkins.¹² More recently, the self-consistent scattered-wave $X\alpha$ approach¹³⁻¹⁵ has been successfully applied to the study of semiconductors containing deep-level impurities.⁵⁻¹⁰ Substitutional transition-metal impurities in silicon have been treated by this method.^{6,7}

In the present investigation, the electronic structure of the neutral interstitial transition-metal impurities, Cr through Ni, is generated by the spin-restricted scattered-wave $X\alpha$ method. A cluster of ten silicon and sixteen hydrogen atoms is assumed with the interstitial impurities located at the geometrical center of the cluster. The sixteen hydrogen atoms serve to terminate the cluster by tying up the silicon dangling bonds. In order to understand how the electronic structure of silicon is altered by the impurity, the calculation is also carried out for the same cluster, but with the impurity absent.

In Sec. II, we discuss the model for the substitutional and interstitial impurities proposed by Ludwig and Woodbury¹ based on their observations. The details of the present calculation for the interstitial impurities are described in Sec. III and the results in Sec. IV. Section V contains a discussion of these results.

II. MODEL

The electron paramagnetic resonance studies of Ludwig and Woodbury¹ provide most of what is known about the transition-metal impurities in silicon. The iron-group transition-metal elements which have been identified as isolated substitutional or interstitial impurities are indicated in Fig. 1. Ludwig and Woodbury have developed a model for the electronic structure of these impurities which is consistent with their observations. The essential features of the model are also indicated in Fig. 1. According to the model, when the impurity is located at the *substitutional* site, four of the transition-metal electrons are involved in bonding. The remaining electrons outside the $n=2$ shell (i.e., $n>2$) occupy the $3d$ level which is split into e and t_2 states by the tetrahedral crystal field. The *interstitial* position is also characterized by tetrahedral symmetry and the $3d$ level is split as before; however, the sign of the crystal field is reversed with t_2 below e . In this case, electrons are not required for bonding and, according to the model, all $n>2$ electrons are contained in the $3d$ shell. For both the substitutional and the interstitial impurities, the single-particle levels are populated according to Hund's rules; i.e., the high-spin state is favored.

The many-electron state associated with each transition-metal impurity can be characterized by the quantum numbers, S , L' , and J , where S represents total spin, and L' and J are effective orbital angular momentum and effective total angular momentum and effective total angular

momentum, respectively. The effective orbital angular momentum is quenched by the crystal field in all of the configurations considered except $3d^6$ and $3d^7$; in these two cases, orbital degeneracy associated with the partially filled t_2 states remains. The g values associated with these two configurations contain both orbital and spin contributions. However, the EPR measurements reveal that the orbital contribution is reduced considerably from the free-atom value ($g_L \ll 1$). In addition, there is a sizable reduction in the spin-orbit constant associated with these impurities. These observations are consistent with hybridization of the transition-metal orbitals with the surrounding ligands. The dynamic Jahn-Teller effect also provides an explanation for these observations.¹⁶ Both the Jahn-Teller effect and covalency may be participating in this reduction, but it is not known which predominates.

The essential features of Ludwig and Woodbury's model for the interstitial are summarized below:

- (i) all $n>2$ electrons contained in the $3d$ shell,
- (ii) $3d$ level split with t_2 below e ,
- (iii) high-spin states favored (Hund's rule),
- (iv) orbital angular momentum and spin-orbit interaction strongly reduced.

III. CALCULATION

The cluster chosen to represent pure crystalline silicon consists of a cage of ten silicon atoms centered on the interstitial position and surrounded by sixteen hydrogen terminators. There are two

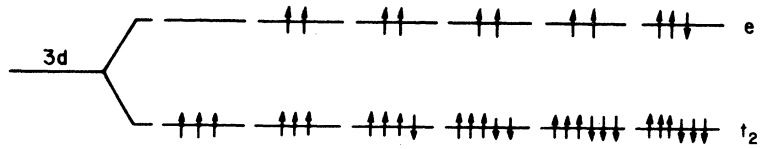
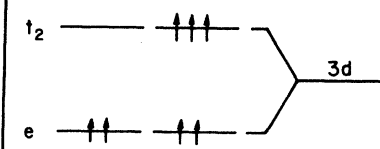
	INTERSTITIAL						SUBSTITUTIONAL	
OBSERVED:	V^{2+}	Cr^{+}, Mn^{2+}	Cr° Mn^{+}	Mn° Fe^{+}	Fe° Mn^{-}	Ni^{+}	Cr° Mn^{+}	Mn^{2-}
OCCUPANCY:	d^3	d^5	d^6	d^7	d^8	d^9	d^2	d^5
								
S	$3/2$	$5/2$	2	$3/2$	1	$1/2$	1	$5/2$
L'	0	0	1	1	0	—	0	0
J	$3/2$	$5/2$	1, 2, 3	$1/2, 3/2, 5/2$	1	$1/2$	1	$5/2$

FIG. 1. Transition-metal ions which have been observed by electron paramagnetic resonance in silicon and corresponding model for the electronic structure. The symbols S , L' , and J represent total spin, effective orbital angular momentum, and effective total angular momentum, respectively (after Ludwig and Woodbury, Ref. 1, p. 266).

shells of silicon atoms (four and six atoms in each) and two shells of hydrogen atoms (four and twelve atoms in each) as shown in Fig. 2. The distance between nearest neighbors is taken as that appropriate to the pure crystal with $r_0 = 4.444a_0$. The hydrogen terminators serve to tie up the dangling bonds and effectively eliminate spurious surface levels from the valence band and from the band gap. The interstitial impurity is represented by this cluster with the appropriate transition-metal element placed at the center.

The electronic structure of the molecular cluster is calculated according to the spin-restricted scattered-wave $X\alpha$ method of Johnson and Smith.^{13,17} Since this method has been discussed at length elsewhere,^{14,15} only a brief summary will be given here. The atoms which form the cluster and the entire cluster itself are surrounded by nonoverlapping spheres, thereby partitioning space into three regions: atomic, interatomic, and extramolecular. The wave function is expanded in a set of partial waves within each region. The eigenvalues and wave functions are determined by the condition that the wave functions and logarithmic derivatives be continuous across all boundaries. The potential energy is represented by a muffin-tin approximation where the potential is spherically averaged in the atomic and extramolecular regions and volume averaged in the interatomic region. The exchange term is approximated by the Slater statistical exchange with α given by Schwarz.¹⁸ The process of generating wave function, then potential is carried to self-consistency.

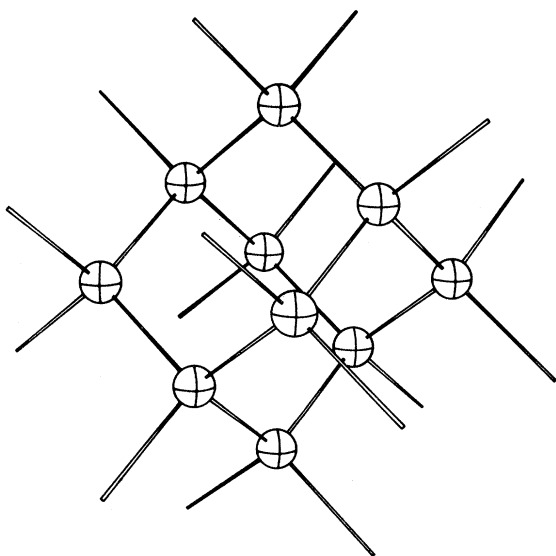


FIG. 2. $\text{Si}_{10}\text{H}_{16}$ cluster centered on the interstitial position. Hydrogen terminators are not shown, but belong at the end of each dangling bond.

In the present calculation, partial waves up to $l=2$ are employed in the transition-metal and extramolecular¹⁹ regions, up to $l=1$ in the silicon regions, and up to $l=0$ in the hydrogen regions. The atomic- and outer-sphere radii are chosen so that the spheres touch but do not overlap; i.e., $r_{\text{atomic}} = 2.221a_0$ and $r_{\text{outer}} = 11.110a_0$. The value of α appropriate to silicon is used for the hydrogen terminators.⁵ The maximum relative difference, $\Delta V/V$, between successive potentials provides a measure of self-consistency. We require that this parameter be less than one percent before the iterative sequence is terminated. After convergence has been achieved for one transition-metal impurity, this potential is used as a starting point for the next element in the transition-metal series.

IV. RESULTS

The electronic structure associated with the cluster $\text{Si}_{10}\text{H}_{16}$ as calculated by the scattered-wave $X\alpha$ method with an empty sphere at the center is shown in Fig. 3(b). The results of the calculation are consistent with experiment [see Figs. 3(a) and 3(b)]. A gap of 0.84 eV is found to separate the occupied and unoccupied single-particle levels. For a very large cluster, this quantity would correspond to the band gap of bulk silicon,¹² which is measured to be 1.16 eV. The width of the occupied valence states is 10.4 eV; the experimental valence-band width for bulk silicon is $\sim 12\text{--}13$ eV.²⁰

It is instructive to characterize the states of the $\text{Si}_{10}\text{H}_{16}$ cluster in the central interstitial region. The t_2 and e states are of particular importance since, by symmetry considerations, they are permitted to interact with the $3d$ states of the transition metal when it is inserted into that position. The degree to which they interact will depend upon the amount by which the t_2 and e states overlap with the transition-metal $3d$ states. This is indicated in Fig. 3(c). Here, we have taken as a measure of the overlap the fractional d -like ($l=2$) character of the t_2 and e states of the $\text{Si}_{10}\text{H}_{16}$ cluster in the empty central-sphere region, i.e., the square of the d projection of each state integrated over the central sphere. Since our interest lies in localized states formed in the forbidden gap, the cluster orbitals of importance are those close to the band edges. It is clear from the figure that the $4t_2$ and $2e$ states are the valence-band states of primary importance. In addition, it will be shown that the $5t_2$ state is also important, by virtue of its interaction with the $4t_2$ state.

The principal results of the present calculation are contained in Fig. 4. We begin with Ni on the left since it has a closed-shell configuration. We note that the energy-level structure remains es-

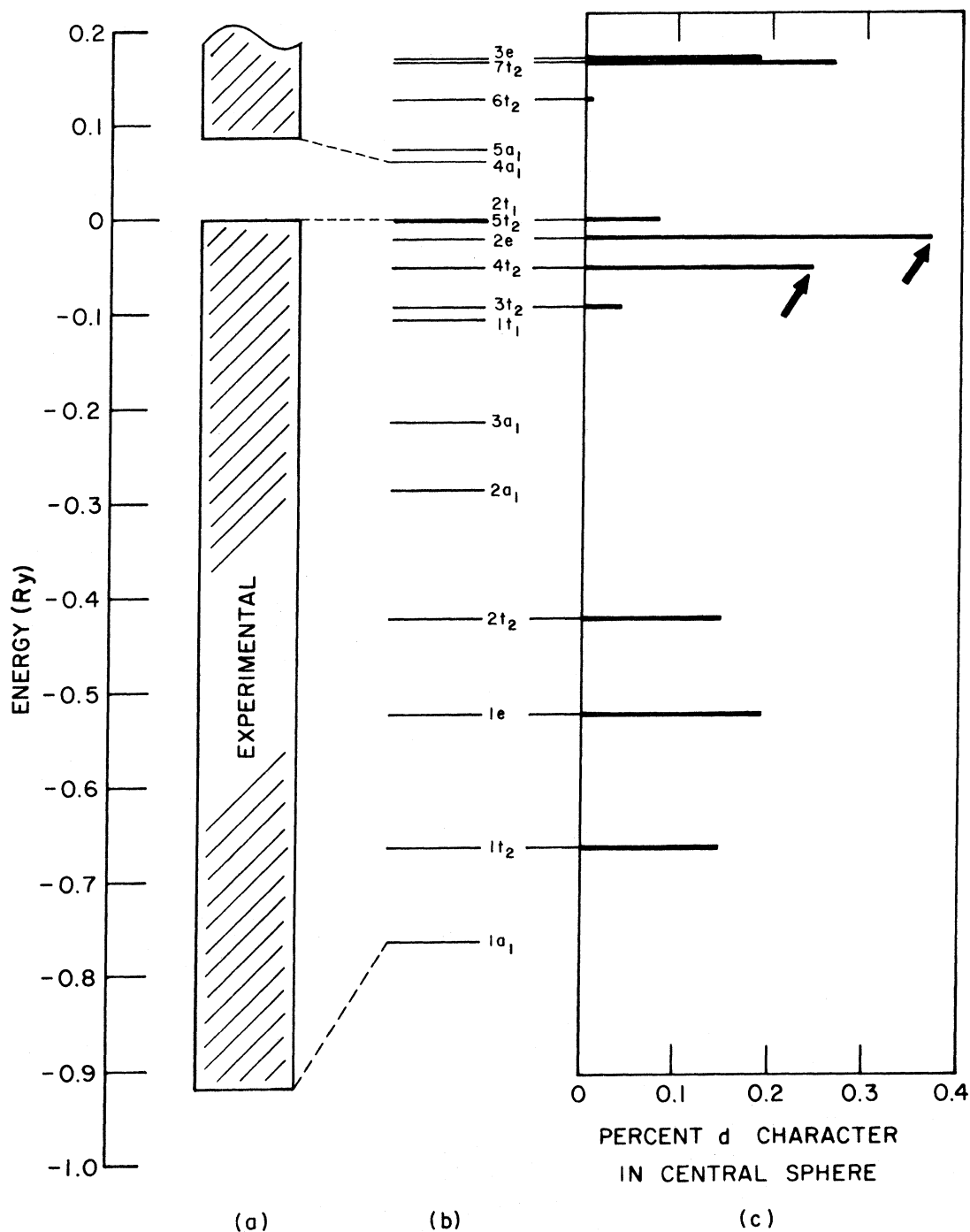


FIG. 3. Calculated electronic structure of $\text{Si}_{10}\text{H}_{16}$ cluster (b) and corresponding d -like character of t_2 and e symmetry states in the central sphere (c); i.e., the square of the d ($l=2$) projection of each state integrated over the central sphere (sum over all l values and all spheres yields 100 for each state). Arrows indicate t_2 and e states with greatest d -like character. The experimentally determined band gap and valence-band width are indicated (a).

essentially unaltered by the presence of the Ni impurity, aside from the appearance of the filled levels labeled dt_2 and de . These levels are evidently derived from the compact and fully occupied Ni $3d$

state. A departure from the unperturbed electronic structure occurs when Ni is replaced by Co. Electrically active deep levels are created as $5t_2$ and $2e$ are pushed up into the band gap. This is

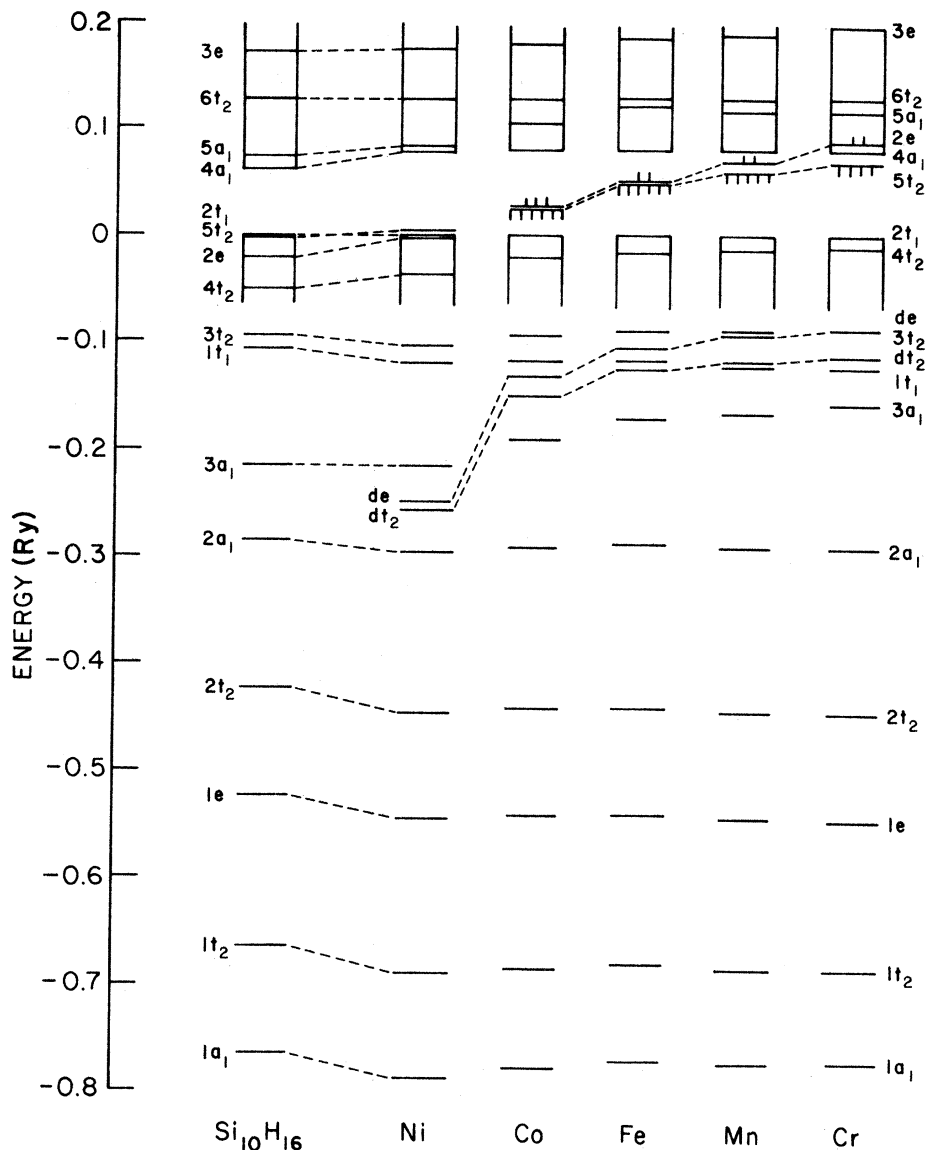


FIG. 4. Calculated electronic structure of $\text{Si}_{10}\text{H}_{16}$ cluster containing Ni, Co, Fe, Mn, and Cr interstitial impurities. No more than one level of each symmetry is shown above the conduction-band minimum ($4a_1$).

accompanied by a large upward displacement of the dt_2 and de levels. This process continues as we move backwards in the transition-metal series until Cr is reached when the $5t_2$ and $2e$ levels begin to move into the conduction band. It is noted that for the transition-metal impurities, Co through Cr, the $5t_2$ level remains below $2e$.

It is instructive to monitor the charge distribution associated with electrons in the states dt_2 , de , $4t_2$, $5t_2$, and $2e$. The corresponding fractional charge contained within the central transition-metal atomic sphere for each single-electron state is shown in Fig. 5(a). This can be considered to represent the fractional amount of time spent by a

single electron in this region for each orbital.

Again starting with Ni, the electrons in states $4t_2$, $5t_2$, and $2e$ have the itinerant character of band-state electrons while those occupying the dt_2 and de states are highly localized on the Ni atom.

The dt_2 and de levels are essentially atomic Ni d states. When Ni is replaced by Co, the dt_2 and de electrons begin to delocalize while $5t_2$ and $2e$ assume a greater transition-metal character. This trend continues through the transition-metal series. As the states dt_2 and de lose their transition-metal character in going from Ni to Cr, they delocalize onto the neighboring silicon atoms. Specifically, the dt_2 electrons spread primarily onto

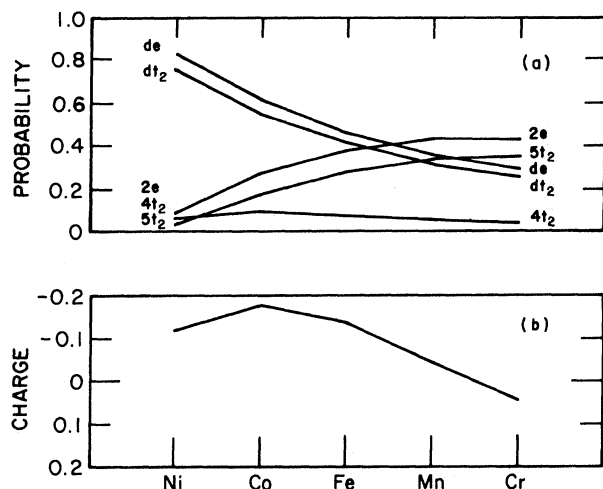


FIG. 5. Uppermost curves (a) represent the probability of finding an electron in the transition-metal sphere for each of the states indicated. The lower curve (b) represents the total charge (all electrons plus nucleus) in this same region.

the four tetrahedrally coordinated silicon atoms, the de states onto the six remaining octahedrally coordinated silicon atoms. Conversely, as the states $5t_2$ and $2e$ gain transition-metal character in going from Ni to Cr, they become less silicon-like. The total amount of charge (electronic plus nuclear) in the impurity sphere is indicated in Fig. 5(b). It is noted that even though the transition-metal $3d$ states become strongly delocalized (dt_2 and de), the total charge remains relatively constant.

A spin-unrestricted calculation was attempted for the $\text{CrSi}_{10}\text{H}_{16}$ cluster, but it failed to converge. The maximum relative difference between successive potential energies ($\Delta V/V$) provides a measure of self-consistency. The divergence was realized when this parameter froze at about two percent while the spin-up and spin-down levels continued to move apart. This effect has been observed by other investigators for substitutional Cr and Fe in InP (Ref. 21) and GaAs.⁸ Although this divergence is not fully understood, it has been suggested that the hydrogen terminators are involved.⁸ In an attempt to investigate this point, the spin-up and spin-down potentials in the hydrogen spheres were replaced by the corresponding averages of the two spins. Although the silicon valence-band states stabilized, the dt_2 , de , $5t_2$, and $2e$ states continued to split even after the relative difference between successive potentials froze at about one percent. A further investigation of this effect is in progress.

V. DISCUSSION AND CONCLUSIONS

The present calculation predicts an energy-level structure which is consistent with the model proposed by Ludwig and Woodbury.¹ Our results support the identification of neutral Cr, Mn, and Fe as interstitial impurities²² and indicate that Co is also a candidate for electrical activity. In all cases, the calculation supports the sign of the crystal field as proposed with the t_2 level located below the e level. A previous calculation predicted an inverted ordering.² Since no state of a_1 symmetry is produced in the gap or valence band, we conclude that the $4s$ states of interstitial $3d$ transition-metal ions are energetically unfavorable with the result that all of the $n > 2$ electrons occupy the $3d$ states. This is in agreement with the model of Ludwig and Woodbury. Finally, the delocalization associated with the partially filled $5t_2$ and $2e$ levels in the gap is consistent with the observed reduction of the orbital angular momentum.

Since the spin-unrestricted calculation failed to converge, the Hund's-rule occupancy observed by Ludwig and Woodbury could not be verified. Therefore, the observed occupancy represents input to our spin-restricted calculations. It is noted, however, that in the spin-unrestricted calculation, the energy-level structure did predict a Hund's-rule occupancy up to the stage where the potential-difference self-consistency parameter, $\Delta V/V$, froze at a constant value. Beyond this, the levels continued to spread into the valence and conduction bands.

The energy-level positions may be interpreted on the basis of ligand-field theory. The transition-metal $3d$ states are expected to interact primarily with the $3p$ states on the ten silicon atoms which surround the interstitial. In particular, a set of σ -type (pointing toward the center) t_2 orbitals may be constructed from p functions centered on the four tetrahedrally coordinated silicons. Similarly, p functions on the nearby set of six octahedrally coordinated silicons provide a σ -type e orbital. As demonstrated by Fig. 3(c), the σ orbitals of primary concern can be associated with the $4t_2$ and $2e$ states of the $\text{Si}_{10}\text{H}_{16}$ cluster. When Ni is introduced into the $\text{Si}_{10}\text{H}_{16}$ cluster, bonding and antibonding t_2 and e states are produced. The bonding levels are denoted dt_2 and de in Fig. 4; the antibonding levels are represented by the states $4t_2$ and $2e$. As a consequence of the large energy difference between the Ni $3d$ and cluster $4t_2$ and $2e$ states, the $4t_2$ and $2e$ levels are not perturbed significantly by the interaction. When Ni is replaced by Co, the dt_2 and de states rise substantially and the $3d$ levels begin to hybridize with the surrounding ligands. The $2e$ level is forced upward into the

gap. The $4t_2$ level starts upward but through its interaction with the $5t_2$ level forces it, in turn, into the gap. The $5t_2$ and $2e$ levels therefore represent the antibonding states resulting from the interaction of the transition-metal $3d$ state with silicon levels near the top of the valence band. This process continues through the transition-metal series as indicated in Fig. 6. The $4t_2$ level lies below the $2e$ level in the $\text{Si}_{10}\text{H}_{16}$ cluster and this ordering of levels, transmitted to the $5t_2$ level, prevails throughout the transition-metal series. It is noted, however, that the crystal-field splitting approaches zero for interstitial Co and Fe (see Figs. 4 and 6). This may be partially an artifact of our finite-sized cluster in which $4t_2$ has a level of the same symmetry located above it in the valence band while $2e$ does not. The $5t_2$ deep level in the impurity cluster approaches the $2e$ level since it is pushed up indirectly, via the $4t_2$ level. In a more realistic calculation (larger cluster), numerous t_2 and e states would be expected above $4t_2$ and $2e$ so that states of both symmetries could be pushed up indirectly. This could serve to increase the crystal-field splitting. However, since there will always be more localized t_2 than e states, this effect near Co and Fe will probably remain to some degree.

As indicated in Fig. 1, the transition-metal interstitials have been observed in a variety of charge states. A number of factors determine whether a given charge state is stable. Starting

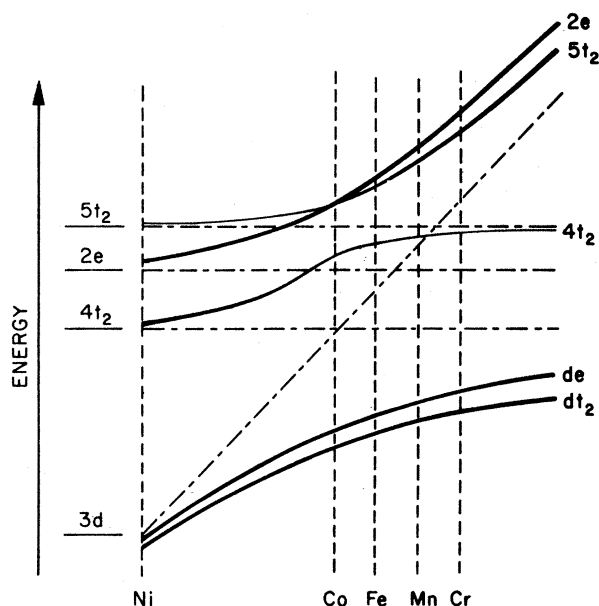


FIG. 6. Schematic representation of ligand field description of bonding and antibonding levels for Cr through Ni interstitials in Si. The thicker lines indicate a relatively large transition-metal character.

with the neutral charge state, electrons may be added, creating acceptor levels, or removed, creating donor levels. Two factors which limit the number of electrons which can be accepted or donated are the crystal field and exchange interactions which provide a stability for filled and half-filled t_2 and e levels. Also, since levels move up (down) when electrons are added (removed), there will be only a limited number of stable states before a partially filled level enters the conduction (valence) band. Haldane and Anderson²³ have considered this effect, concluding that the magnitude may be reduced significantly from the atomic values by hybridization with band states. In this paper, we have performed single-particle-state calculations for the neutral defect only. However, considering the above factors, they can serve as a rough guide to the stability of the other charge states as well. For instance, if the lowest partially occupied level is close to the conduction band, as in the case of Cr^0 , an acceptor level (Cr^-) is not expected. A single donor level is expected, however, corresponding to the removal of the spin-down electron (see Fig. 1) from the partially filled t_2 state. This is confirmed experimentally by the EPR observations of both Cr^0 and Cr^+ . Further donor action is less likely because the next electron must come from the more stable (Hund's rule) half filled e state. The lowest partially filled state for Mn^0 is somewhat lower in energy explaining the existence of a single acceptor level (Mn^- is stable). On the other hand, the Mn^0 level is still fairly high in the gap allowing for the two observed donor levels associated with the removal of the two spin-down electrons from the t_2 state. The highest occupied orbital for Fe^0 is still lower in energy. At least one donor state (confirmed by the stability of Fe^+) is expected.

We see that for these ions, the multiple donor and acceptor action (experimentally verified for Cr, Mn, and Fe) are simply related to the filling and emptying of the partially occupied spin-down t_2 states. Mn is most strategically located in the gap so that all of the available states from Mn^- ($t_2^{1/3}$) to Mn^{2+} ($t_2^{4/0}$) are stable. This general feature is borne out in our calculation, the average (spin-up and spin-down) t_2 state for neutral Mn^0 being in the upper half of the gap. The arguments that we have developed would predict no other charge states for Ni; however, Ni^+ is observed but occupying a distorted lattice site. In general, Jahn-Teller distortions can also stabilize different charge states. In addition, this stability could reflect the raising of the $2e$ spin-down level into the gap by the exchange splitting.

Unfortunately, there appear to be few, if any, reliable measurements at present for the electri-

cal level positions in the gap associated with these interstitial ions to which we can compare our results. This is primarily because the interstitial ions are fast diffusers in the lattice and defect pairing clouds the interpretation of the measurements. There does seem to be a reasonable consensus developing, however, that the single donor state of Fe may be at $E_V + 0.4$ eV.²⁴ This is in fair agreement with our result which locates the donating $5t_2$ level at 0.68 eV above the filled $2t_1$ level of the cluster.

To make a more proper connection to the donor level position, a transition-state calculation should be made which, for a very large cluster, would correspond to a calculation with a half-electron removed from the $5t_2$ level. (This is a statement of the failure of Koopmans's theorem for our single-particle-state calculation.) This would lower the predicted donor level position in the gap somewhat. On the other hand, a properly converged spin-unrestricted calculation would raise the level because the electron is being removed from the minority (lower occupancy) spin-down state. These refinements are being explored and will be the subject of subsequent publications.

In summary, the present calculation predicts electrically active levels deep within the band gap for neutral interstitial Cr, Mn, Fe, and Co. Physically, they arise from t_2 and e orbitals, localized primarily on the nearest- and next-nearest-neighbor silicons, that are close to the top of the valence band which are pushed up into the gap in the presence of the interstitial $3d$ ion. The t_2 level is located below the e level in all cases, consistent with the model of Ludwig and Woodbury.

ACKNOWLEDGMENTS

The authors would like to thank Dr. R. P. Messmer and Dr. D. R. Salahub for providing us with a version of the scattered-wave $X\alpha$ program and assistance in operating it. We also thank A. Edwards for the computer-generated image of our cluster shown in Fig. 2. The authors are grateful for the generous amount of computer time and assistance which was made available by the Lehigh University Computer Center. This research was supported by the U. S. Navy Office of Naval Research Electronics and Solid State Science Program Contract No. N00014-76-C-1097.

¹G. W. Ludwig and H. H. Woodbury, *Solid State Phys.* **13**, 263 (1962).

²A. B. Roitsin and L. A. Firshtein, *Fiz. Tverd. Tela (Leningrad)* **13**, 63 (1971) [*Sov. Phys. Solid State* **13**, 50 (1971)].

³J. Bernholc and S. T. Pantelides, *Phys. Rev. B* **18**, 1780 (1978).

⁴G. A. Baraff and M. Schlüter, *Phys. Rev. B* **19**, 4965 (1979).

⁵B. G. Cartling, *J. Phys. C* **8**, 3171 (1975).

⁶B. G. Cartling, *J. Phys. C* **8**, 3183 (1975).

⁷L. A. Hemstreet, *Phys. Rev. B* **15**, 834 (1977).

⁸L. A. Hemstreet and J. O. Dimmock, *Phys. Rev. B* **20**, 1527 (1979).

⁹A. Fazzio and J. R. Leite, *Phys. Rev. B* **21**, 4710 (1980).

¹⁰A. Fazzio, M. J. Caldas, and J. R. Leite, *Int. J. Quant. Chem.* **S13**, 394 (1979).

¹¹S. T. Pantelides, M. Scheffler, J. Bernholc, and N. O. Lipari, *Bull. Am. Phys. Soc.* **25**, 290 (1980).

¹²R. P. Messmer and G. D. Watkins, *Phys. Rev. B* **7**, 2568 (1973).

¹³K. H. Johnson and F. C. Smith, Jr., *Phys. Rev. B* **5**, 831 (1972).

¹⁴J. C. Slater, *The Self-Consistent Field for Molecules and Solids* (McGraw-Hill, New York, 1974).

¹⁵K. H. Johnson, in *Advances in Quantum Chemistry*, edited by P. O. Löwdin (Academic, New York, 1973), Vol. 7, p. 143.

¹⁶F. S. Ham, in *Electron Paramagnetic Resonance*, edited by S. Geschwind (Plenum, New York, 1972).

¹⁷ $X\alpha$ computer program written by F. C. Smith, Jr. and K. H. Johnson, MIT, Cambridge, MA.

¹⁸K. Schwarz, *Phys. Rev. B* **5**, 2466 (1972).

¹⁹A limited amount of central memory has prevented us from using more partial waves in the extramolecular region. This restriction has been investigated by reducing the number of partial waves in the central sphere to $l=0$ for $\text{Si}_{10}\text{H}_{16}$ permitting an increase in the extramolecular region to $l=3$. The differences between the $l=2$ and 3 calculations were found to be insignificant.

²⁰W. D. Grobman and D. E. Eastman, *Phys. Rev. Lett.* **29**, 1508 (1972).

²¹L. A. Hemstreet, private communication.

²²Although the $2e$ state of the Cr cluster is located above the unoccupied $4a_1$ state, this presents no difficulty since a cluster calculation is not expected to accurately predict the positions of conduction-band states (note that we calculate a band gap which is too small). In addition, a proper spin-unrestricted calculation would be expected to yield an occupied $2e$ level lowered into the gap by exchange splitting.

²³F. D. M. Haldane and P. W. Anderson, *Phys. Rev. B* **13**, 2553 (1976).

²⁴E. Weber and H. G. Riethe, *Appl. Phys. Lett.* **33**, 433 (1978).